Development of high power, InP-based quantum cascade lasers on alternative epitaxial platforms

Steven Slivken, Nirajman Shrestha, Manijeh Razeghi*

Center for Quantum Devices, Department of Electrical and Computer Engineering, Northwestern University, Evanston, IL 60208, USA

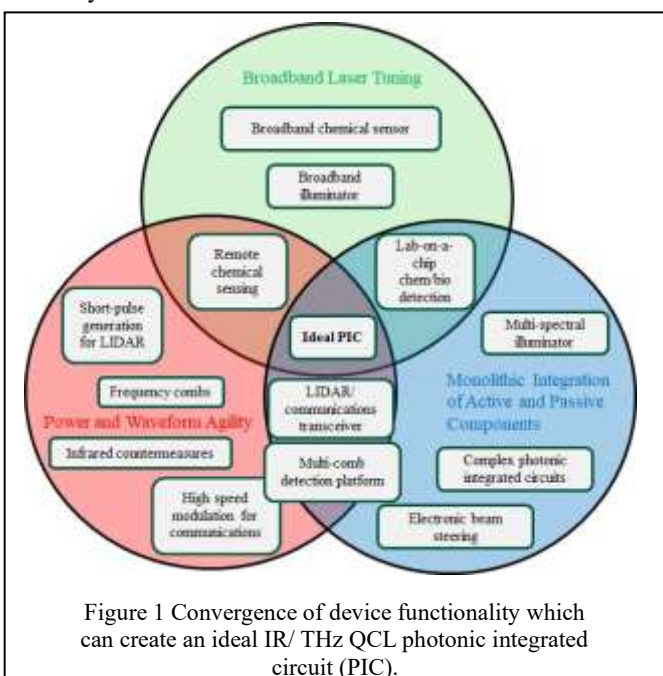
ABSTRACT

In this talk, challenges and solutions associated with the monolithic, epitaxial integration of mid- and longwave- infrared, InP-based quantum cascade lasers on GaAs and Si wafers will be discussed. Initial results, including room temperature, high power, and continuous wave operation, will be described.

Keywords: Quantum cascade laser, heteroepitaxy, monolithic integration

1. INTRODUCTION

The quantum cascade laser (QCL) is an attractive technology for a variety of applications from mid-infrared to THz spectral regions. High power, high speed modulation, and wide wavelength tuning are key elements which could be utilized. However, most of the QCL development to date has been related to discrete devices, which is not ideal for an integrated systems approach. From a manufacturing perspective, a primary goal should be monolithic integration of devices and to eliminate as many external optical components as possible. This can significantly reduce system size, weight, and power (SWaP). In addition, production on a wafer scale can also reduce costs associated with component production and assembly.



A key element for this approach is transitioning active device manufacturing technology to larger, less expensive wafers. This not only provides the opportunity of larger dies for more sophisticated photonic integrated circuits, but also provides a general economy of scale for discrete devices, especially if discrete device performance is comparable to devices on native substrates. Si wafers are perhaps one the best potential options, based both on the maximum wafer diameter (450 mm) and the mature photonics technologies already developed on this platform.

Hybrid integration of lasers via wafer bonding to Si is a popular approach for interband lasers, QCLs, and interband cascade lasers (ICLs) [1,2,3,4], but, unfortunately, it is not easily scalable. Most commercial QCLs are grown on 50-75 mm InP wafers. Even assuming that this process could scale to 150 mm InP wafers, multiple wafers would be required to cover the whole Si wafer, and there would be a low fill factor. Further, the overall performance of hybridized QCLs at

this point is far below the performance of discrete QCLs.

Direct bonding of discrete QCLs onto Si waveguides is another option, but requires individual device alignment with sub-micron accuracy. This is also not easily scalable to large wafers.

^{*} email: razeghi@eecs.northwestern.edu; phone: 1-847-491-7251; http://cqd.eecs.northwestern.edu

Quantum Sensing and Nano Electronics and Photonics XX, edited by Manijeh Razeghi, Giti A. Khodaparast, Miriam S. Vitiello, Proc. of SPIE Vol. 12895, 1289503 © 2024 SPIE · 0277-786X · doi: 10.1117/12.3009335

One promising and more straightforward approach to integrate QCLs directly onto Si wafers is through direct growth (heteroepitaxy). Multiple hurdles exist, however, due to significant mismatch in crystal lattice constant and thermal expansion coefficients. This most often leads to the presence of a large density of dislocations in the crystal. Despite these difficulties, functional InP-based (interband) diode lasers have been produced this way by multiple groups [5,6]. Nevertheless, these interband lasers often exhibit decreased performance and/or lifetime compared to devices on native substrate.

Unlike traditional interband diode lasers, which are minority carrier devices, the QCL is an intersubband device based on majority carrier transport. As such, the presence of crystalline dislocations have a potentially much weaker impact on device operation [7]. The device is sensitive to surface quality, though, as it is composed of several hundred layers only a few atoms thick. Provided a smooth and monocrystalline InP-on-Si template can be grown, it is feasible to produce QCLs on Si with nearly the same performance as the same structure grown on an InP wafer. This paper will review some of the recent progress in this area which has come a long way towards establishing this new technology.

2. INP-BASED QCLS GROWN ON GAAS

Though growth of InP-based QCLs on Si is the eventual goal, an intermediate step is to grow them first on GaAs, which has approximately half the lattice mismatch (4%). In addition, both substrate and epilayers have the same, zinc blende, symmetry, which simplifies the nucleation of the mismatched film. Though multiple groups made attempts to realize this intermediate demonstration, Northwestern was the first to demonstrate multi-Watt peak power output at room temperature [8], using a combination of metalorganic chemical vapor deposition (MOCVD) and gas-source molecular beam epitaxy (GSMBE) growth techniques.

The MOCVD method was first used to grow a metamorphic InP template layer directly on an n+, exact-oriented (001) GaAs wafer. An abrupt transition was made to n-InP, in order to minimize cross-hatching, which is often exacerbated when using a graded composition buffer layer. The rms roughness of the surface after template growth was only 1.2 nm over a $10 \ \mu m \times 10 \ \mu m$ area, as measured by an atomic force microscope (AFM). GSMBE was used to grow the QCL active layers, based on a strain-balanced shallow-well design [9]. Following GSMBE growth, an upper n-InP cladding and a n+ InP cap layer are grown using MOCVD. The final wafer had a rms roughness below 2 nm.

A piece of the wafer was fabricated into double channel waveguide QCLs. This simple process used wet etching to define a central waveguide of 25 μ m width. A top metal contact was used to inject current into the center of the laser waveguide. A second contact was made to the bottom of the thinned (200 μ m) n+ GaAs wafer. For testing, laser bars of 3, 4, and 5 mm were cleaved, and the mirror facets were left uncoated. Laser bars were mounted epilayer-up with indium to copper heat sinks. Laser testing was conducted in pulsed mode using 200 ns pulses at a repetition rate of 100 kHz. Further fabrication and testing details can be found in Ref. 8.

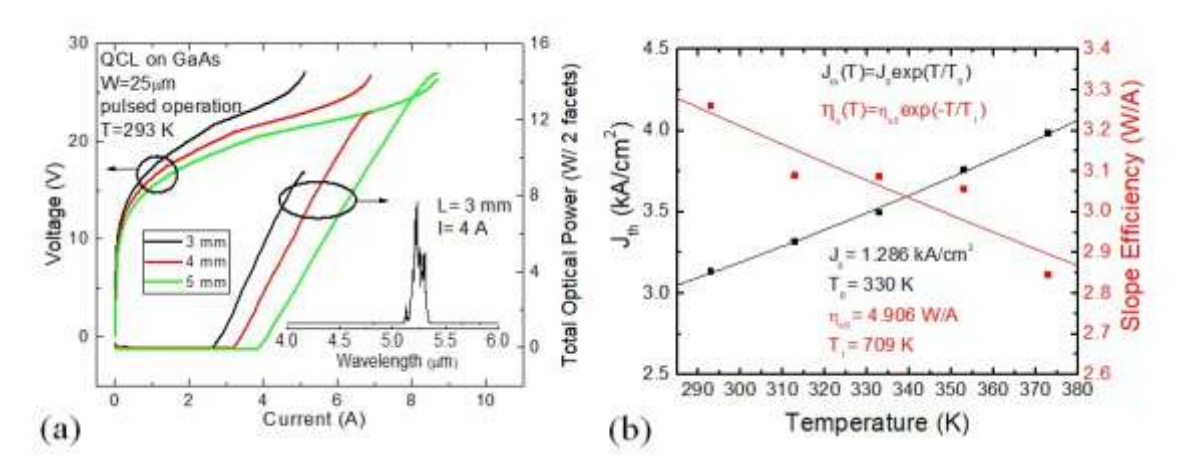


Figure 2 (a) Electrical and output power characteristics for different cavity lengths as a function of current. Inset shows emitting spectra of the 3 mm long laser at a pulsed current of 4 A. (b) Plot of extracted J_{th} and η_s data as a function of temperature for the 5

mm cavity. Solid lines represent exponential fits to the data.

Power and voltage as a function of current for the different cavity lengths are shown in Figure 2a. The 5 mm long cavity exhibited a threshold current density (J_{th}) of 3.13 kA/cm² with a total peak power up to 14.5 W. The wallplug efficiency is similar for all cavity lengths with a maximum value of 7.2% obtained for the 5 mm long cavity. This is hampered

primarily by the use of a bottom contact directly on the GaAs substrate. Though simple to process and functional, this geometry is not ideal due a significant added voltage/ series resistance present at the GaAs/InP interface. It is estimated that the intrinsic device efficiency would be \sim 50% higher when paired with lateral current injection, as will be described in the following section.

The temperature dependence of the laser performance was also measured, up to a temperature of 373 K ($100 \,^{\circ}$ C), as shown in Figure 2b. The threshold and slope efficiency (η_s) trends were fit to exponential functions, giving characteristic temperatures of 330 K and 709 K, respectively. This low temperature sensitivity suggests that the laser band structure, designed to minimize thermal leakage and parasitic relaxation, can be maintained for InP-based QCLs grown on GaAs.

Following this demonstration, an independent verification of InP-based QCLs grown by metalorganic vapor phase epitaxy (MOVPE) on GaAs substrate was published as well [10]. The QCL devices in this reference are also strain-balanced and emit at a wavelength of 5.7 µm. Laser performance, though not as good as demonstrated above, is similar to that of lasers of the same design grown on native InP.

3. INP-BASED QCLS GROWN ON SILICON

Efforts to grow QCLs directly on Si has only seen success in the last 5 years. Inspiration for our recent efforts include the very low threshold current density ($< 1 \text{ kA/cm}^2$) obtained at room temperature for a λ ~8 μ m InAs-based QCL grown on Si [11]. As InAs is even more mismatched than InP, this work certainly showed proof-of-concept, but was not focused on high power or continuous wave (CW) operation. At that time, InP-based realizations were limited to cryogenic operation [12].

The situation changed in 2022, when our group developed an InP-on-Si template suitable for QCL growth using GSMBE [13]. This template incorporates an abrupt GaAs/Si buffer with thermal cycle annealing, followed by an abrupt transition to InP. In addition, a 5 nm/5 nm $Ga_{0.467}In_{0.533}As$ / InP superlattice (SL) is used as a dislocation filter prior to growing a thicker bulk InP layer. The template is visually smooth, with a rms roughness of 1.88 nm measured by atomic force microscopy over a 100 μ m² area. The (004) x-ray diffraction spectrum of the template is shown in Figure 3, and the Si, GaAs, and InP layers are clearly observed. The full width at half maximum (FWHM) of the three peaks are 19, 372, and 280 arcsec, respectively. The full structure has an estimated dislocation density of $5.3x10^8$ cm⁻².

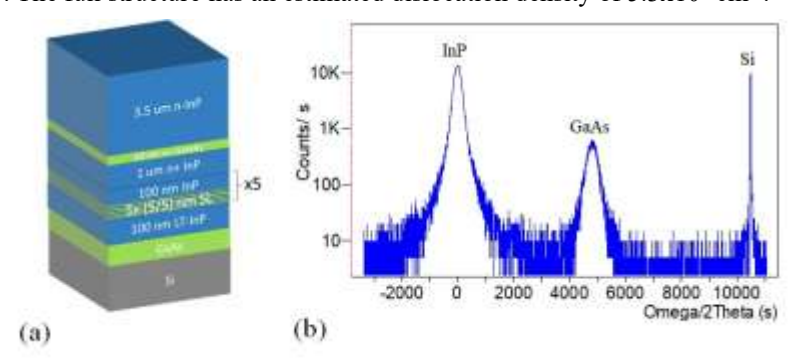
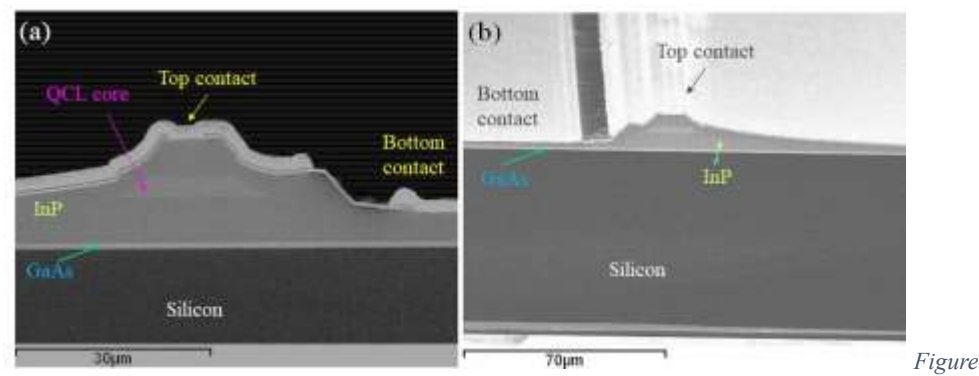


Figure 3 (a) Layer sequence of InP-on-Si template. (b) (004) x-ray diffraction spectrum of InP-on-Si template.

Two separate QCL demonstrations were made using this template initially. The first was based on a lattice-matched $Ga_{0.467}In_{0.533}As/Al_{0.478}In_{0.522}As$ superlattice designed for an emission wavelength of~10 µm [14]. A lattice-matched core (50-stage) was chosen to avoid potential lattice relaxation that may occur on the InP-on-Si template surface, which is rougher than a typical InP substrate (rms roughness < 0.2 nm). In addition, the laser core doping was fairly high in order to favor high power pulsed operation in the event that cavity losses were high or the material differential gain was low.

Realizing that the vertical injection structure had significant excess voltage drop, bottom contact layers were integrated into the InP-on-Si template which facilitates the use of two contacts on the epitaxial side of the wafer. This avoids extra resistance through the heterointerfaces and makes the process inherently compatible with the use of high resistivity Si or silicon-on-insulator (SOI) wafers in the future.

The LWIR wafer was processed into a buried heterostructure waveguide with a core width of $18~\mu m$. As mentioned above, a lateral injection scheme was used, where current travels vertically through the laser core from a top contact on top of the waveguide to a bottom contact which is ~25 μm away from the laser core and is connected to a n+ InP layer in the template. A cross sectional SEM image of the LWIR laser is shown in Figure 4a.



4 SEM images of buried heterostructure QCLs grown on Si substrates. (a) LWIR laser. (b) MWIR laser.

Lasers were tested in pulsed mode (200 ns pulses @ 250 kHz) and operated easily up to 373 K. With a cavity length of 5 mm, up to 4 W of peak power was observed, with a threshold current density of 7.44 kA/cm². The emission wavelength was 10.8 μ m, which is only 9.2 meV shifted compared to the design. This may be attributed in part to a 3% error in

was $10.8 \mu m$, which is only 9.2 meV shifted compared to the design. This may be attributed in part to a 3% error in thickness, which was observed from x-ray analysis. In addition, the operating voltage of these lateral injection lasers was significantly reduced compared to the vertical injection scheme, and the I-V characteristic as similar to that of QCLs grown on InP.

The second demonstration made was based on a strain-balanced QCL core (40-stage) with same nominal structure as used for the above demonstration on GaAs. Compared to the lattice-matched wafer, there was some additional roughness. Though this may be related to additional strain relaxation within the laser core, structural characterization was not conclusive. Similar to the LWIR wafer, the MWIR wafer was processed into a buried heterostructure waveguide with a core width of 18 µm. An SEM image of the completed device is shown in Figure 4b.

High peak power (4.5 W) operation was observed for a cavity length of 8 mm at 120 K. Both uncoated and HR-coated lasers showed >1 W peak power output at room temperature, with the HR-coated laser delivering up to 1.6 W. The emission wavelength was 4.82 μ m at room temperature. The threshold current density of the uncoated and HR-coated lasers are 4.6 and 4.2 kA/cm², respectively. This is significantly higher than the lasers grown on GaAs, but was an excellent initial result. The variation in threshold current density for the two laser cavities suggests a differential modal gain of ~2 cm/kA, which is about 62% of the value obtained for the laser grown on GaAs.

While both of these initial experiments were helpful in establishing room temperature operation of InP-based QCL on Si, neither was especially promising for CW operation. For this to happen, it is crucial that two things happen. First, the operating power density must be reduced. This can be done by a combination of realizing lower losses, increasing the differential gain, and lowering the laser core doping density. Second, the thermal impedance of the device must be reduced by optimizing the laser geometry.

With respect to the first requirement, it is critical to choose a laser design with high differential gain. This is related to both laser design and material quality. While optimizing material quality in the future will definitely help, in the near term, we decided to first focus on design. The best performing QCLs in both the MWIR and LWIR and currently based on strainbalanced heterostructures. Despite the potential issue with strain relaxation suggested above, it is really the only sustainable choice if the MWIR spectral range needs to be accessed. Next, the specific core design needs to be chosen to exhibit high modal differential gain. In some cases, this can be accomplished simply by increasing the number of cascade stages, which was employed in the LWIR demonstration to follow. In the MWIR range, though, we chose both a larger number of emitting stages and an older emitter design with a higher natural differential gain.

In addition, the laser geometry was modified to support both a narrower laser core and a more planarized surface above the laser core. The former step directly increases thermal conductance, which the latter step was done to improve the waveguide performance and make the laser more suitable for epilayer-down bonding [15]. Shown in are SEM images of the new laser geometry, as fabricated on a Si substrate.

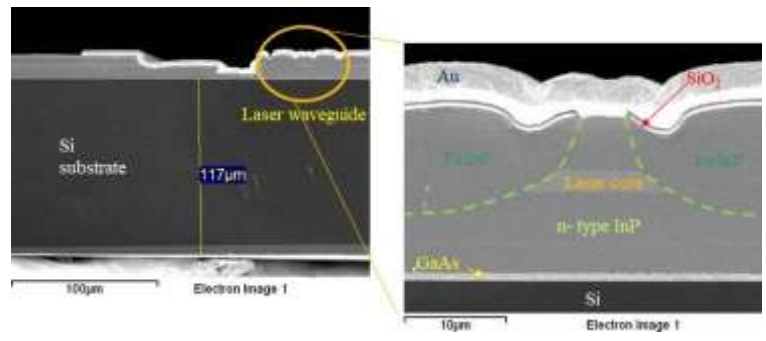


Figure 5 Cross-sectional image of QCL waveguide, showing the planarized Fe:InP regrowth, lateral contact scheme, and Si substrate thickness.

A strain-balanced MWIR laser (λ -4.75 µm) with a high differential gain was grown first at Northwestern. Similar to before, the template and laser core were grown by GSMBE, and the upper cladding and cap layers were grown by MOCVD. The number of stages in the laser core was increased to 50, and the core width was chosen to be 6 µm. For a 5 mm, uncoated laser cavity length, the threshold current density was only 1.89 kA/cm² at room temperature, with a total peak output power of ~2 W (per 2 facets) and a wallplug efficiency of 9.5%. Compared to the previous MWIR demonstration, this is a ~3x reduction in threshold current density. This is comparable to QCLs grown directly on InP and is a very good candidate for CW operation with further development.

If we focus now on LWIR QCLs, it should be noted that there have been some promising room temperature, pulsed demonstrations of InP-based QCLs grown on Si in the past year by other groups. This includes a lattice matched, $\lambda \sim 11.5$

 μ m laser core with a J_{th} of 4.3 kA/cm² and a wallplug efficiency of 3% [16]. This laser was grown on a Ge/Si template using MBE. Another recent effort utilized a commercial GaP/Si template, on which a GaAs buffer was grown by MBE, followed by all MOCVD growth of an InP-based template and the QCL [17]. In this effort, the core was also lattice matched, targeting an emission wavelength of \sim 8.5 μ m. A J_{th} as low as 1.5 kA/cm² was achieved, with a wallplug efficiency of 2.85%. Even more incredible was the comparative testing of the same laser core grown on a native InP substrate, which showed similar performance. While the latter demonstration has good potential for CW operation, the device geometry was not engineered for high thermal conductance.

At Northwestern, a 50-stage, strain-balanced LWIR laser core was also grown in the past year on the GSMBE InP-on-Si template, utilizing a state-of-the-art emitter design published earlier [18]. The waveguide core width was chosen to be 11 μ m. Excellent pulsed performance was also seen for this wafer, with a pulsed wallplug efficiency of 11.1% and a pulsed emission wavelength of ~8.3 μ m [19]. This is an improvement of about 5x compared to the previous LWIR demonstration made by our group. The J_{th} for this laser was as low as 1.3 kA/cm² with an operating voltage of 10.5-13 V. All figures of merit are notably better than seen in previous publications.

In addition to pulsed testing, these QCLs on Si also operated in CW mode at room temperature, which has not been observed before. At room temperature, over 0.7 W of output power was observed, with operation up to 348 K, as shown in Figure 6a. It should be noted that these lasers were bonded epilayer-side up on copper submounts, with no special packaging. With epilayer down bonding and high fidelity packaging, the performance is expected to be significantly enhanced. The beam shape for this initial demonstration was mainly single lobed, but had some minor instability with current, as shown in Figure 6b. While not optimal, the angular width did not exceed 1.45 times the diffraction limit. This can be corrected by optimizing the laser geometry to suppress higher order lateral waveguide modes.

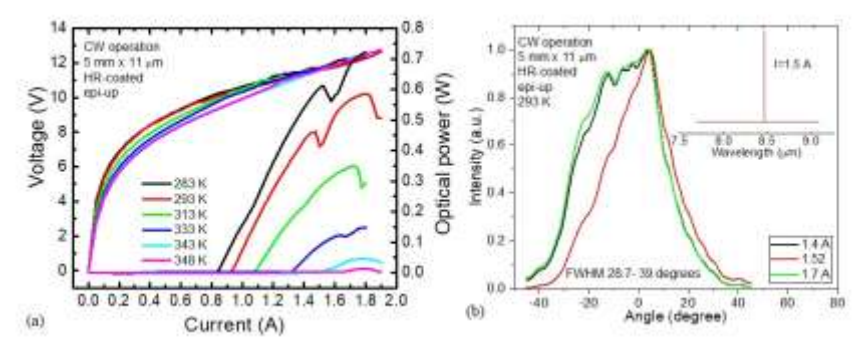


Figure 6 (a) Epilayer-up continuous wave voltage and power output as a function of current for different heat sink temperatures. (b) Far field intensity distribution parallel to the wafer plane at several currents. Inset shows emitting spectra at 1.5 A.

4. FUTURE OUTLOOK

Thanks to the experimental demonstrations shown above, it is becoming evident that direct growth of intersubband devices (such as QCLs) is a very real, emerging technology. The devices operate very well, despite a large density of dislocations (10⁸-10⁹ cm²) present. If this technology expands to larger diameter Si wafers and industrial-scale fabrication, it is likely that we can expect significant savings in laser cost in the years to come, especially for pulsed devices. For CW QCLs, QCL-on-Si reliability should be investigated to see if the presence of dislocations has any significant effect on QCL lifetime.

It should also be noted that THz QCLs also have a strong potential for direct integration on Si. This includes both direct emission devices as well as those based on intracavity difference frequency generation [20]. For the latter, some effort was put into wafer bonding InP devices onto high resistivity Si substrate for reduced losses. With this direct growth technology, however, this device geometry becomes incredibly straightforward.

Another active area of investigation currently is the integration of MWIR and LWIR lasers with Si planar lightwave circuits. Previously this was limited to hybrid integration on a small scale. Direct growth technology opens up many new possibilities here as well, including optimization of light transfer, massively parallel integration of laser arrays on large diameter (>150 mm) wafers, development of integrated detection capability, and process refinement for integration with electronic circuits.

5. ACKNOWLEDGEMENTS

This material is based upon work supported by the Naval Air Warfare Center Weapons Division, China Lake, CA under Contract No N6893622C0023. This work is also partially supported by the National Science Foundation under Grant No. ECCS-2149908.

REFERENCES

[1] Sun, X., Zadok, A., Shearn, M. J., Diest, K. A., Ghaffari, A., Atwater, H. A., Scherer, A., Yariv, A., "Electrically pumped hybrid evanescent Si/InGaAsP lasers," Opt. Lett. 34(9), 1345-1347 (2009), doi: 10.1364/OL.34.001345. [2] Spott, A., Peters, J., Davenport, M. L., Stanton, E. J., Merritt, C. D., Bewley, W. W., Vurgaftman, I., Kim, C. S., Meyer, J. R., Kirch, J., Mawst, L. J., Botez, D., Bowers, J. E., "Quantum cascade laser on silicon," Optica 3, 545-551 (2016), doi: 10.1364/OPTICA.3.000545.

- [9] Bai, Y.; Bandyopadhyay, N.; Tsao, S.; Slivken, S.; Razeghi, M., "Room temperature quantum cascade lasers with 27% wall plug efficiency," Appl. Phys. Lett. 98, 181102 (2011).
- [10] Xu, S., Zhang, S., Gao, H., Kirch, J., Botez, D., Mawst, L., "Strain-balanced InGaAs/AlInAs/InP quantum cascade laser grown on GaAs by MOVPE," J. Cryst. Growth 619, 127310 (2023).
- [11] Tournié, E., Bartolome, L. M., Calvo, M. R., Loghmari, Z., Díaz-Thomas, D. A., Teissier, R., Baranov, A. N., Cerutti, L., Rodriguez, J. -B.," Mid-infrared III–V semiconductor lasers epitaxially grown on Si substrates," Light: Science & Applications 11, 165 (2022), doi: 10.1038/s41377-022-00850-4.

^[3] Coutard, J.G., Brun, M., Fournier, M., Lartigue, O., Fedeli, F., Maisons, G., Fedeli, J. M., Nicoletti, S., Carras, M., Durafourg, L., "Volume Fabrication of Quantum Cascade Lasers on 200 mm-CMOS pilot line," Sci. Rep. 10, 6185 (2020), doi: 10.1038/s41598-020-63106.

^[4] Spott, A., Stanton, E. J., Torres, A., Davenport, M. L., Canedy, C. L., Vurgaftman, I., Kim, M., Kim, C. S., Merritt, C. D., Bewley, W. W., Meyer, J. R., Bowers, J. E., "Interband cascade laser on silicon," Optica 5, 996-1005 (2018), doi: 10.1364/OPTICA.5.000996.

^[5] Razeghi, M., Defour, M., Blondeau, R., Omnes, F., Maurel, P., Acher, O., Brillouet, F., C-Fan, J. C., Salerno, J., "First cw operation of a $Ga_{0.25}In_{0.75}As_{0.5}P_{0.5}$ – InP laser on a silicon substrate," Appl. Phys. Lett. 53, 2389 (1988), doi: 10.1063/1.100239.

^[6] Shi, B., Han, Y., Li, Q., Lau, K. M., "1.55-μm Lasers Epitaxially Grown on Silicon," IEEE Journal of Selected Topics in Quantum Electronics 25(6), 1900711 (2019), doi: 10.1109/JSTQE.2019.2927579.

^[7] Tournié, E. Bartolome, L. M., Calvo, M. R., Loghmari, Z., Díaz-Thomas, D. A., Teissier, R., Baranov, A. N., Cerutti, L., Rodriguez, J. -B., "Mid-infrared III–V semiconductor lasers epitaxially grown on Si substrates," Light: Science & Applications 11, 165 (2022), doi: 10.1038/s41377-022-00850-4.

^[8] Slivken, S., Razeghi, M., "High Power Mid-Infrared Quantum Cascade Lasers Grown on GaAs," Photonics 9(4), 231 (2022).

- [12] Go, R., Krysiak, H., Fetters, M., Figueiredo, P., Suttinger, M., Fang, X. M., Eisenbach, A., Fastenau, J. M., Lubyshev, D., Liu, A. W. K., Huy, N. G., Morgan, A. O., Edwards, S. A., Furlong, M. J., Lyakh, A., "InP-based quantum cascade lasers monolithically integrated onto silicon," Opt. Exp. 26, 22389-22393 (2018), doi: 10.1364/OE.26.022389.
- [13] Slivken, S., Razeghi, M., "High Power, Room Temperature InP-Based Quantum Cascade Laser Grown on Si," IEEE Journal of Quantum Electronics 58, 2300206 (2022), doi: 10.1109/JQE.2022.3212052.
- [14] Slivken, S., Razeghi, M., "High Power, Room Temperature InP-Based Quantum Cascade Laser Grown on Si," IEEE Journal of Quantum Electronics 58, 2300206 (2022), doi: 10.1109/JQE.2022.3212052.
- [15] Wang, F., Slivken, S., Wu, D. H., Lu, Q. Y., Razeghi, M., "Continuous wave quantum cascade lasers with 5.6 W output power at room temperature and 41% wall-plug efficiency in cryogenic operation," AIP Advances 10, 055120 (2020), doi:, 10.1063/5.0003318.
- [16] Cristobal, E., Fetters, M., Liu, A. W. K., Fastenau, J. M., Azim, A., Milbocker, L., Lyakh, A., "High peak power quantum cascade lasers monolithically integrated onto silicon with high yield and good near-term reliability," Appl. Phys. Lett. 122, 141108 (2023), doi: 10.1063/5.0149072.
- [17] Xu, S., Zhang, Z., Kirch, J. D., Gao, H., Wang, Y., Lee, M. L., Tatavarti, S. R., Botez, D., Mawst, L. J., "8.1 µmemitting InP-based quantum cascade laser grown on Si by metalorganic chemical vapor deposition," Appl. Phys. Lett. 123, 013110 (2023), doi: 10.1063/5.0155202.
- Zhou, W., Lu, Q. Y., Wu, D. H., Slivken, S., Razeghi, M., "High-power, continuous-wave, phase-locked quantum cascade laser arrays emitting at 8 μm," Opt. Exp. 27, 15776-15785 (2019), doi: 10.1364/OE.27.015776.
- [19] Slivken, S., Razeghi, M., "Room Temperature, Continuous Wave Quantum Cascade Laser Grown Directly on a Si Wafer," IEEE J. of Quant. Elect. 59, 2300206 (2023), doi: 10.1109/JQE.2023.3282710.
- [20] Lu, Q. Y., Wang, F. H., Wu, D. H., Slivken, S., Razeghi, M., "Room temperature terahertz semiconductor frequency comb," Nat. Comm. 10, 2403 (2019).